

ALMA 2009 Paper Presentation:

Woofers Design using non-linear BL(x) curves

Drivers can either be designed for target Thiele-Small (TS) parameters or target system response in several ways. The sound quality depends on excursion, shape of the BL(x) curve, Voice Coil offset, amount of steel, compliance linearity, high power stability and so on. In addition there is a demand for cost savings as the material prices have increased drastically.

Practical design examples considering all these aspects will be given.

Design for target TS parameters

An example of a woofer design using target Thiele-Small (TS) parameters is illustrated in this section. The following target specifications are given:

Target Specifications:

Woofers	6.5 inch
Nominal impedance	8 ohms
Total Qts	~0.3-0.35
Resonance frequency F_s	<40 Hz
X_{max}	~5mm
(V_{as}	<40 liters)
Magnetically Shielded	

Available driver components:

1. Voice coil:
 - a. \varnothing 25.60mm ID
 - b. DCR (R_e)=6.2 ohms
 - c. 0.05 mm Kapton former/bobbin
2. 6.5" paper Cone + Sur.:
 - a. 13.11cm diameter
 - b. Cone F_o =22.5 Hz
 - c. (Cone + dust cap + $\frac{1}{2}$ surround + $\frac{1}{2}$ spider =8g)
3. Top plate:
 - a. ID 27.20mm
 - b. 5mm thickness

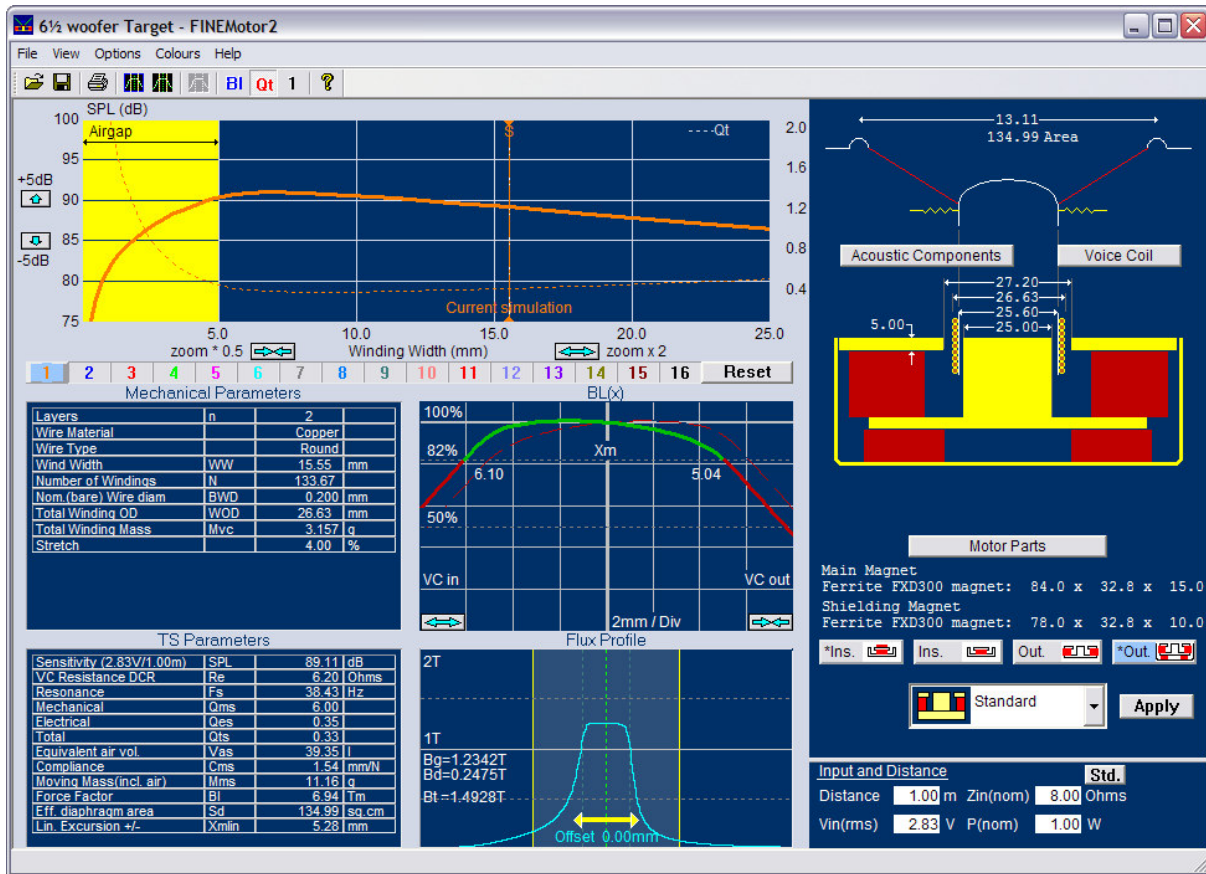


Figure 1 – Initial FINEMotor solution

One solution to satisfy the target specifications is simulated in FINEMotor, shown in Fig. 1: A 2-layer Copper Voice Coil (VC) having a winding width of 15.5mm is centered in the 5mm top plate, and is surrounding a normal straight pole-piece with no extension. The shielded ferrite motor is using an 84x33x15mm magnet.

The calculated TS parameters fit well with the target, giving $Q_{ts}=0.33$ and $F_s \sim 38\text{Hz}$ with a VC overhang of 5.28mm. However all is not perfect, which is illustrated by the BL(x) curve (part of Fig.1). This curve is simulating BL as a function of the VC travel (x), where the green part indicates when $BL > 82\%$ of the value at the resting position, which is the known condition for ensuring low distortion. The dashed red curve is the mirror curve about the vertical axis, and indicates whether BL(x) is symmetric about the Y-axis, corresponding to in/out of the motor system.

In this case the BL(x) curve is reasonably flat, but not symmetric around the Y-axis. In such cases the average Voice Coil position will shift due to the rectifying effect produced by this BL non-linearity. The actual flux profile through the air-gap is shown below, and is clearly not symmetrical, but being higher in the left side. This is caused by the magnetic stray field, which is increased below the air-gap due to the straight pole piece, encouraging the flux lines.

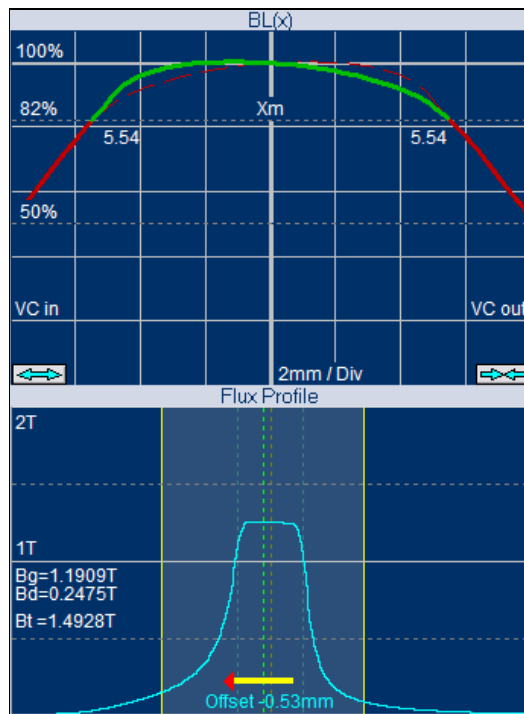


Figure 2 – BL(x) with 0.53mm VC offset

In Fig. 2 the Voice Coil rest position has been moved by dragging the VC 0.53mm into the motor (in the flux profile window), which does increase the symmetry now giving an $X_{max} = 5.54$ mm (at BL(x) = 82%) in both directions. However in such cases a DC offset out of the motor may still happen above F_s . Further improvement will therefore have to include changes to the shape of the flux profile/pole piece.

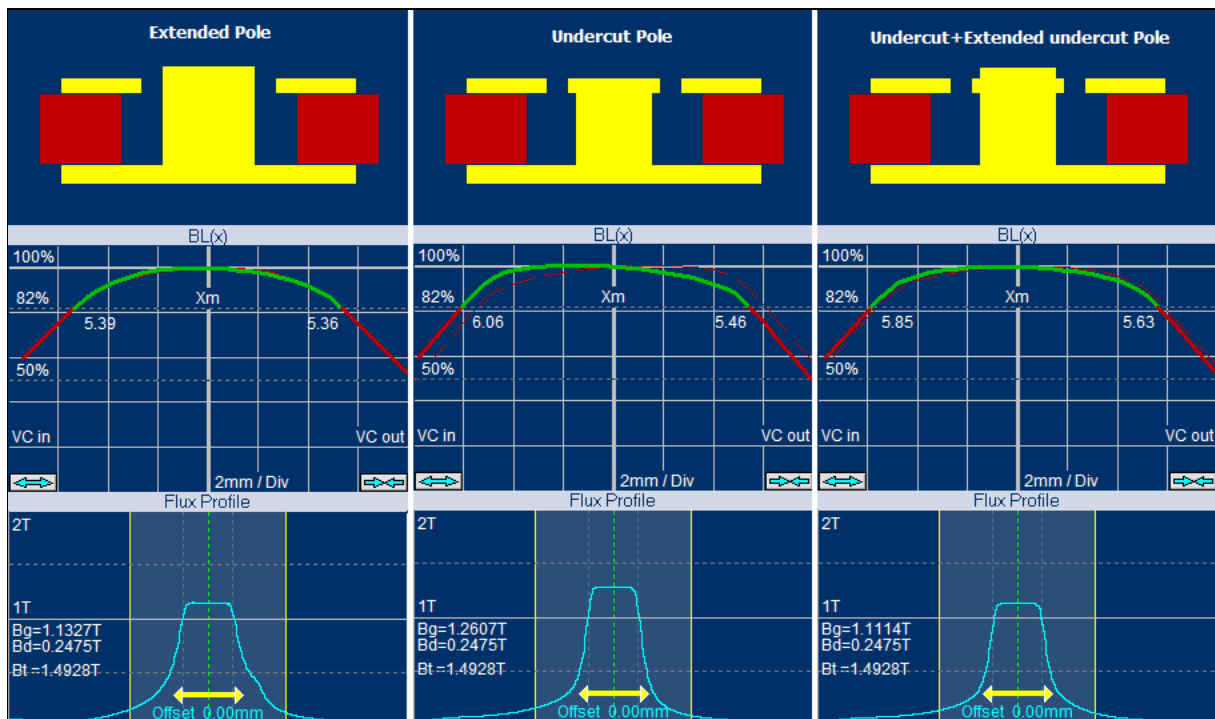


Figure 3 – BL(x) for 3 different Pole Geometries

Fig. 3 gives various ways to modify the geometry of the pole piece. Starting left the pole is here extended to increase the stray field above the top plate, centre is an undercut pole to minimize the stray field below the top plate, and right is a special combination of the two by also undercutting the pole extension.

The extended pole provides a very symmetrical, but not quite flat $BL(x)$ curve and high BL because the stray field is well utilized, see Fig.4 (the flux profile in fig.3 has a "bump" on the right side). The undercut pole concentrates the flux much better in the air-gap, but is not as symmetrical and the BL is lower due to less stray flux. The special undercut combination gives an extremely symmetrical and very flat $BL(x)$ curve, however with a lower BL .

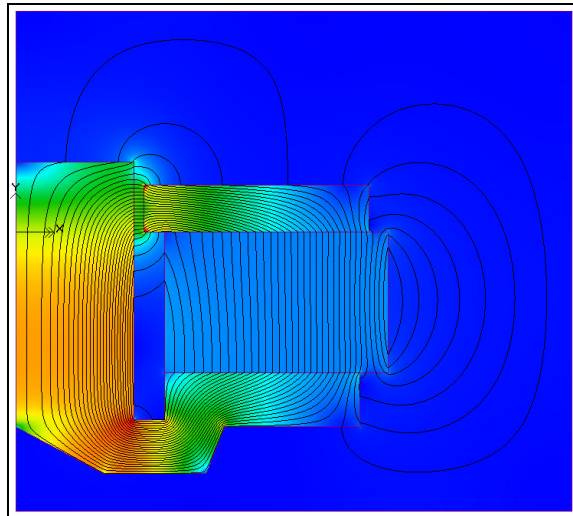


Figure 4 – Magnetic FEA of extended Pole geometry

In this case the extended pole piece is chosen; the pole extension is here 2.5mm, which is half of the top plate thickness. The available maximum VC travel (x), indicated by the green $BL(x)$ part, is 5.36mm (when $BL > 82\%$ of the value at the resting position), which is even slightly more than the linear X_{max} (VC overhang). The calculated TS parameters in Fig.1 are unchanged and fit the target. Shielding was added to the motor, while keeping the same TS parameters.

The maximum flux density in the top plate is 1.49T, which is far from saturation (given by $B_t = 1.49T$ in the flux window). A thinner top plate is possible, but does not give better performance.

Alternative Solution

Other non-linearities for the pole geometry will be considered later, but in the following the woofer is designed for the target specs, using a 4-layer Voice Coil.

The 4-layer wire dimension, VC winding height and number of windings etc. is easily calculated, but the air-gap diameter must be increased to accommodate the larger winding outer diameter. The question is how much.

As a solution it is decided to use the same VC clearance as for the 2-layer VC, and let the software calculate both the new 4-layer VC and the new air-gap flux, and then use those data to calculate the new TS parameters.

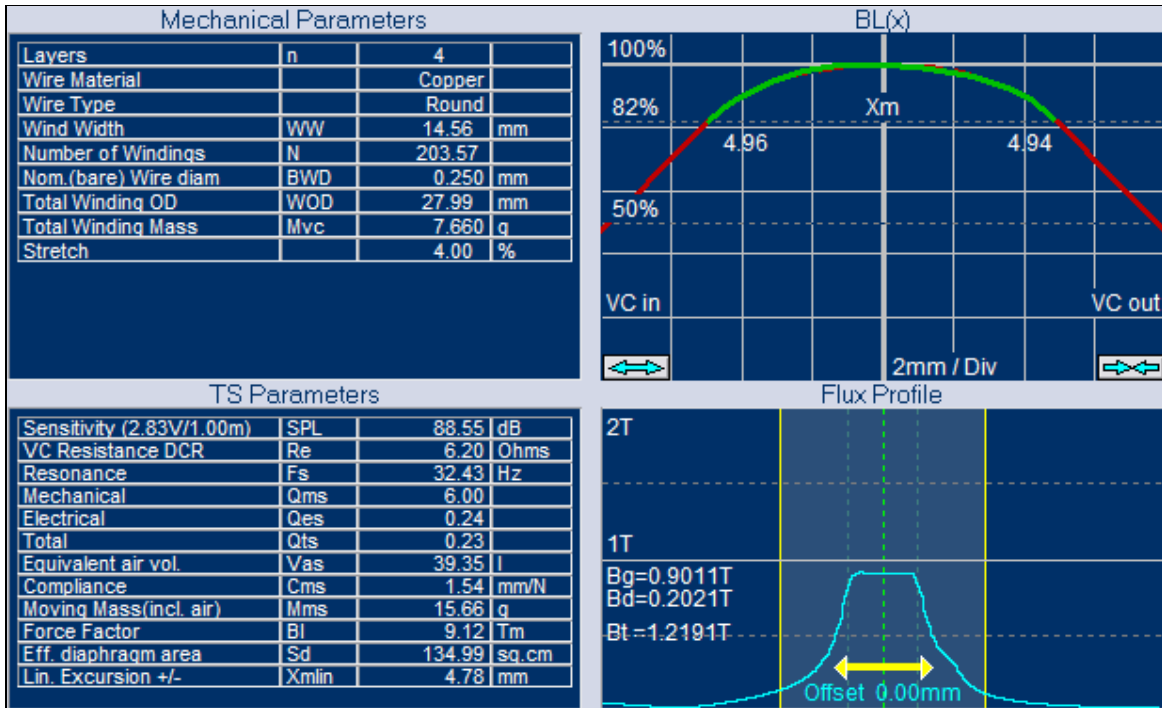


Figure 5 – First calculation with 4-layer VC (Extended Pole)

Fig. 5 gives the Voice Coil winding data for the 4-layer VC in “Mechanical Parameters” and the corresponding calculated TS parameters below. The first observation is $Q_{ts} = 0.23$, which is far too low. F_s is lower due to the increased VC mass. (The magnet operating point given by $B_d = 0.2021T$ also gives reduced low temperature stability)

The reason for the low Q_{ts} is that BL suddenly increased from 6.94 to 9.12Tm, an increase of 31%; despite the much lower flux density in the air-gap (B_g was lowered from 1.23 to 0.9T). The explanation is of course the increased number of windings of the 4-layer VC (203 windings), compared to the 2-layer VC (133 windings), a 73% increase.

An easy fix is therefore to switch to a smaller 72x32x15mm main ferrite magnet (and also a reduced size 60x32x10 shielding magnet) , which will give another solution of TS parameters fitting the target, see Fig. 6 below. Q_{ts} is back to 0.33 caused by a lower BL value of 7.50Tm. The $B_d = 0.2387T$ now indicates good low temperature stability.

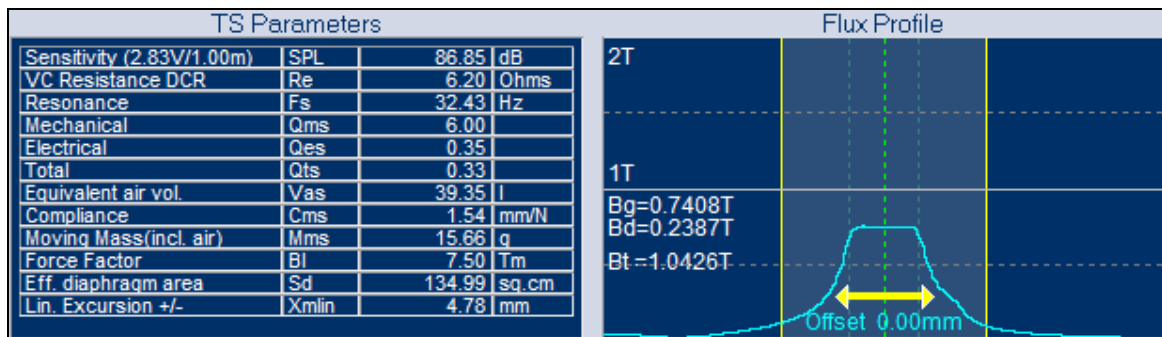


Figure 6 – Final 4-layer VC calculation fitting Target

Fig. 7 gives the new magnet and steel dimensions. The two smaller magnet sizes and correspondingly less steel give a considerable cost saving.

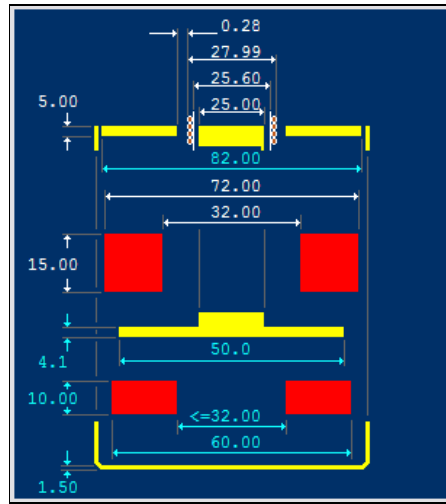


Figure 7 – 4-layer Magnet Parts

Considering that two different solutions to the same target TS parameters have been found, it will be interesting to see how these drivers will perform in the intended 20 liter bass reflex cabinet.

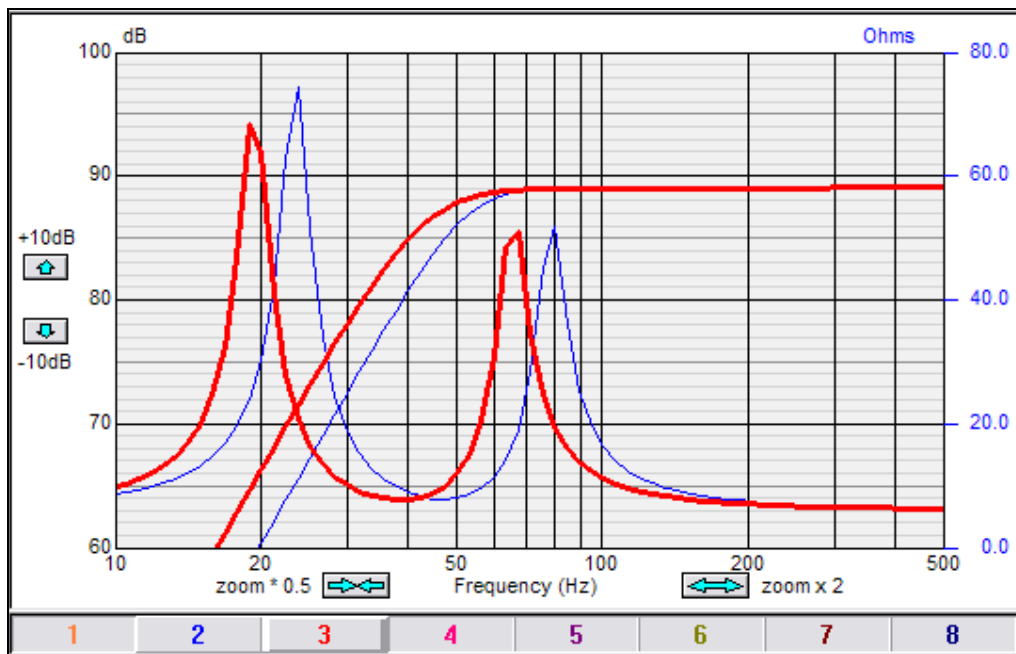


Figure 8- Bass Reflex responses of 2-layer VC ___ / 4-layer VC ___

Fig. 8 shows the response of the two drivers in the 20 liter bass reflex box calculated in FINEBox. The blue response is the first 2-layer VC solution, tuned to $F_b=48$ Hz which produces close to a maximally flat B4 response (actually QB3). The red curve is the second driver solution with the 4-layer VC. In this case a lower tuning frequency $F_b=39$ Hz, gives a similar B4 response, however now with a considerable low frequency extension.

NB the red curve is normalized to the same level by raising it 2.2 dB, to compensate for the lower sensitivity of the 4-layer VC version.

The conclusion is therefore that the 4-layer VC version is attractive due to the low frequency extension and a considerable cost saving, however accepting the 2 dB lower sensitivity, mostly caused by the increased mass. See also later regarding VC inductance.

Compliance

So far only the BL non-linearity has been considered. The two other main driver nonlinearities are compliance and inductance of the Voice Coil.

The total compliance has contributions from both the surround and spider. Usually the spider is much stiffer than the surround (lower spider compliance), and the spider is normally stretching out providing a mechanical limitation of the excursion. A normal half-roll surround is quite linear, but with a relatively sharp increase in stiffness when it reaches its maximum excursion.

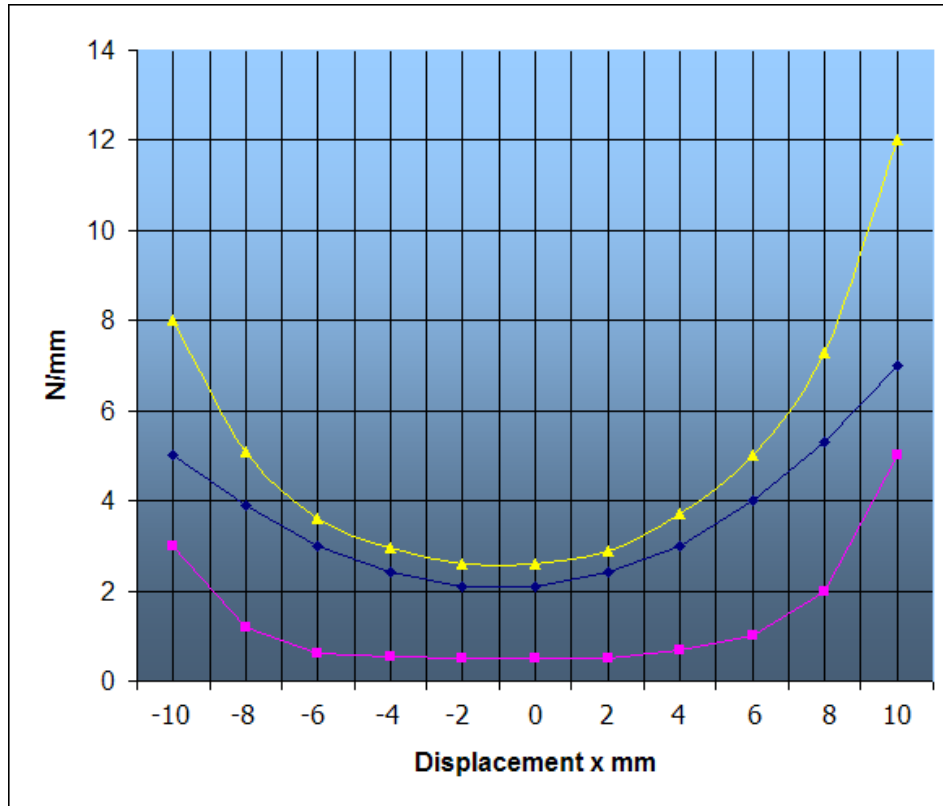


Figure 9 – Stiffness (Spider ___ / Surround ___ / Total ___)

A typical example of suspension stiffness curves is shown in Fig. 9. The blue curve is the spider stiffness and the magenta curve is the surround, being much softer, but increasing very much at maximum negative and positive travel. The total stiffness is shown in yellow.

If the spider is capable of much more excursion than the surround, an annoyingly bad sound may be the result when the surround suddenly is stretching out. Usually the surround is much stronger than the spider, especially a half roll rubber surround, but many designs intentionally use a kind of soft limiting spider, to avoid the sudden sharp sound from the surround.

The symmetry of the compliance is the most important. A symmetrical curve will prevent the rectifying effect which causes a DC-component giving distortion and reducing the useable X_{max} . The spider must be flat, without any cup or similar, as that will exactly produce the offset we are trying to prevent. If a part of the corrugations of the spider is effectively stiffened by glue, the remaining active spider part must be symmetric from that point.

Fig. 10 is an impedance measurement of a small 2.5 inch driver at 3 different input levels: 5, 0.5 and 0.05V. The resonance F_s is seen to vary very much with the input current, which is another effect of the compliance non-linearity.

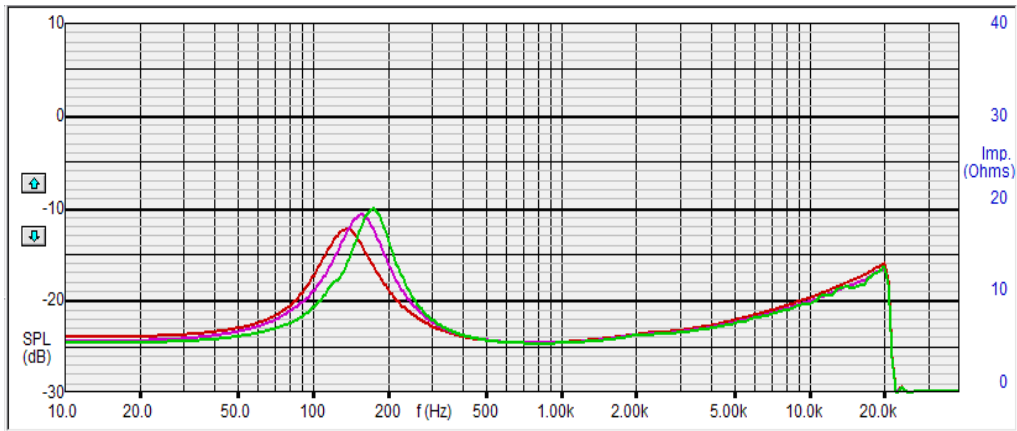


Figure 10 – F_s of 2½ inch driver measured at 5 / 0.5 / 0.05V Input

Q_{ts} is also known to be proportional to the resonance frequency F_s . Despite that it will be relevant to find out what will happen to the low frequency response of the bass reflex system, when F_s is increased by increasing the total stiffness (= reducing the compliance).

Fig. 11 gives the “Acoustic Components” where the current compliances are specified / calculated. The current spider is close to 3 times stiffer than the surround.

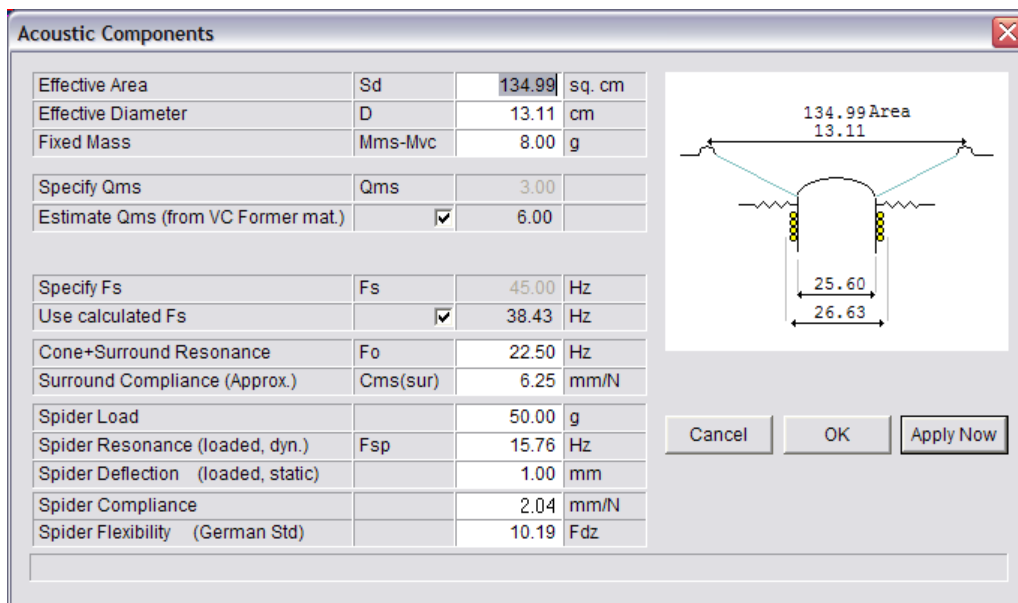


Figure 11 – Compliance / F_s Specification

Fig. 12 shows the response of the 2-layer VC woofer in the 20 liter bass reflex box in blue. The red response is the same driver, but with increased suspension stiffness giving $F_s=55\text{Hz}$ and $Q_{ts}=0.45$, now tuned to $F_b=49\text{Hz}$ to give a very similar response compared to the previous.

The VC excursion is reduced below F_b , giving more stability because the response is controlled by the suspension stiffness in this region.

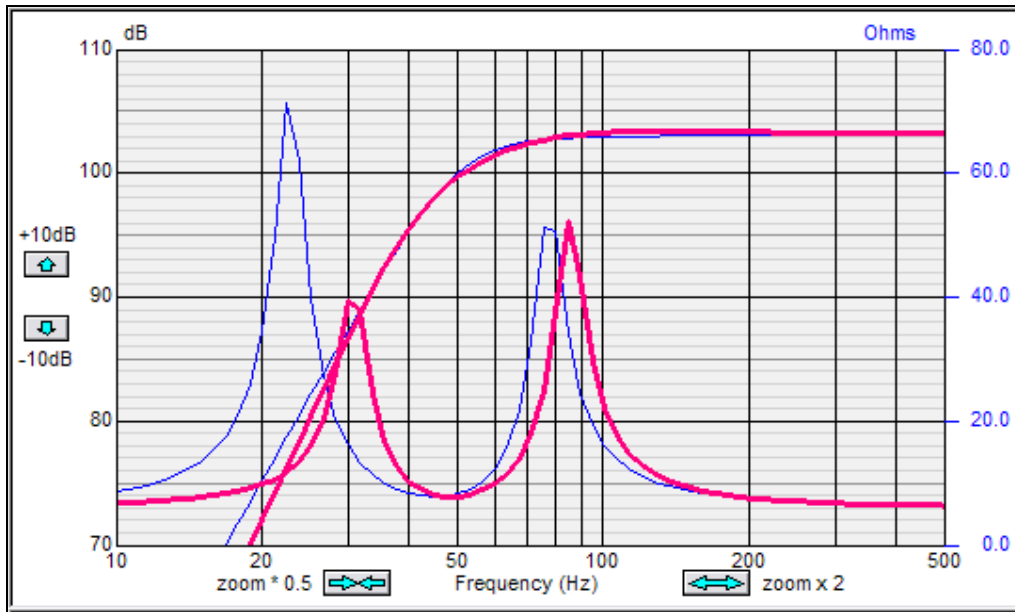


Figure 12 – 2-layer VC woofer in 20L Reflex box ___ Fs=38Hz/ ___ Fs=55Hz

The next Fig. 13 is a good example showing a 6.5inch/165mm woofer with a response problem at 1500Hz. The surround was optimized by increasing the roll thickness, which improved the response and increased the stiffness of the surround at the same time.

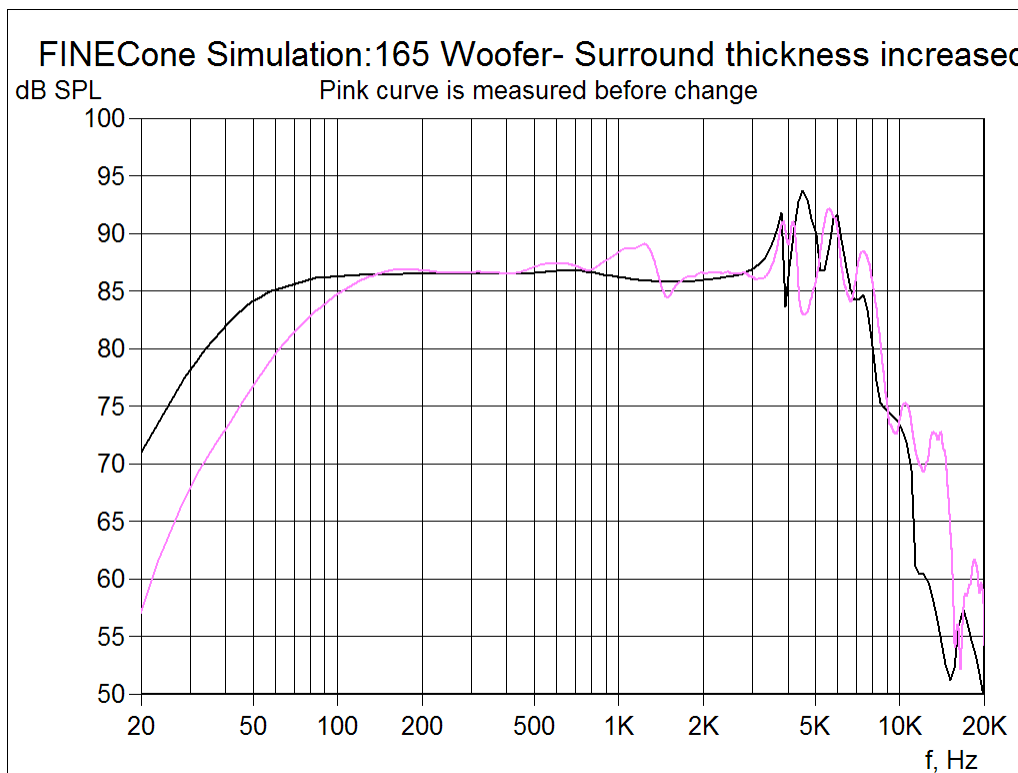


Figure 13 – FINECone Simulation of 6in woofer with changed Surround ___ / standard ___

The conclusion is that the standard Qts and Fs tuning formulas are not always good as a design rule. Simulation gives many more options and the possibility of optimization of components.

Voice Coil Inductance

The basic inductance formula for a cylindrical coil is given:

$$L = \frac{\mu_0 \mu_r N^2 A}{l}$$

L = Inductance in henries (H)

μ_0 = permeability of free space = $4\pi \times 10^{-7}$ H/m

μ_r = relative permeability of core material

N = number of turns

A = area of cross-section of the coil in square metres (m²)

l = length of coil in metres (m)

When designing a driver Voice Coil the diameter and winding width are usually determined by target performance plus power rating and costs. Therefore the designer needs to consider the number of windings and the amount of steel in order to control the VC inductance.

The symmetry of the induction is largely determined by the amount of steel inside the VC, both at rest and at the extreme positions in/out of the air-gap.

In the beginning an extended pole piece was chosen, which will also help to reduce the variation of VC induction, because the amount of steel inside the VC is less dependent on the actual position of the VC. But the steel may also be minimized by undercutting the pole piece under and above the top plate.

Actually an inside magnet/Neodymium motor configuration usually has much less steel close to the VC and therefore less induction making it an interesting solution in many cases, especially with a top neo magnet, see Fig. 14

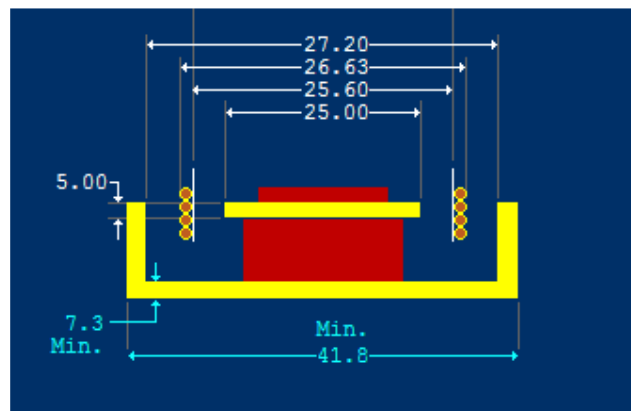


Figure 14 – Inside Neodymium motor with minimum Steel

To illustrate how the inductance varies with VC excursion, the impedance of a woofer having a 4-layer VC and pole piece with no extension or undercut was measured, see Fig. 15. There is a considerable variation of the impedance at mid- and high frequencies, when the VC is moved up/down in the gap, which is a significant source of distortion.

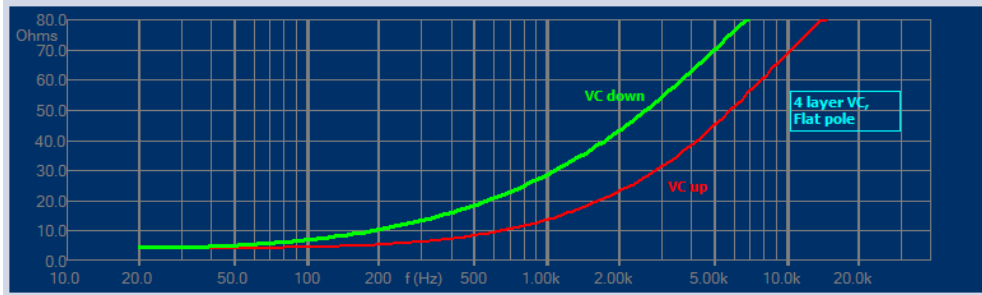


Figure 15 – Measured 4-layer VC Woofer Impedance, VC up / down

The next Fig. 16 shows the measured impedance of a woofer having a 2-layer VC, undercut pole and a flat spider. The little difference between VC up and down promises low distortion.

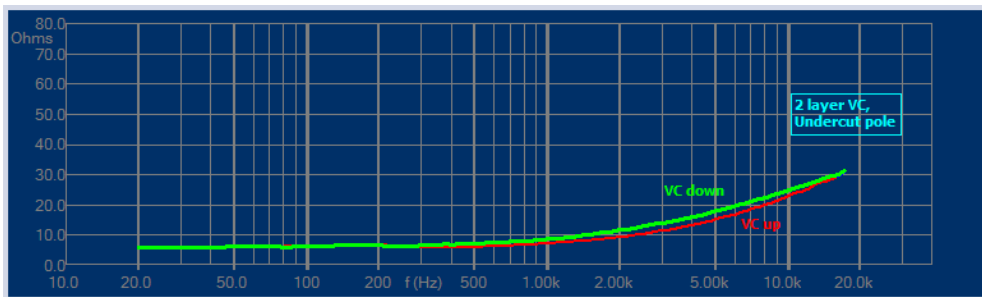


Figure 16 - Measured 2-layer VC Woofer Impedance, VC up / down

In the inductance formula the number of windings is squared (N^2), indicating that this factor has the greatest influence on the inductance. This could also explain why the 2-layer VC has less inductance. The 4-layer VC had 203 windings compared to the 2-layer VC with just 133 windings.

Therefore there exists another method to decrease the VC inductance. The normal Voice Coil winding using round wires is only effectively using a part of the space occupied by the winding. A square wire will in theory come close to 100%. A real flat wire Voice Coil will still have a comparatively higher BL, and less windings, especially when wound in 1 layer with a rather flat wire, see the sketch in Fig. 17.

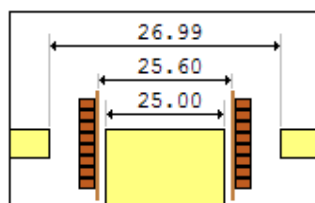


Figure 17 – 1-layer Flat Wire Voice Coil

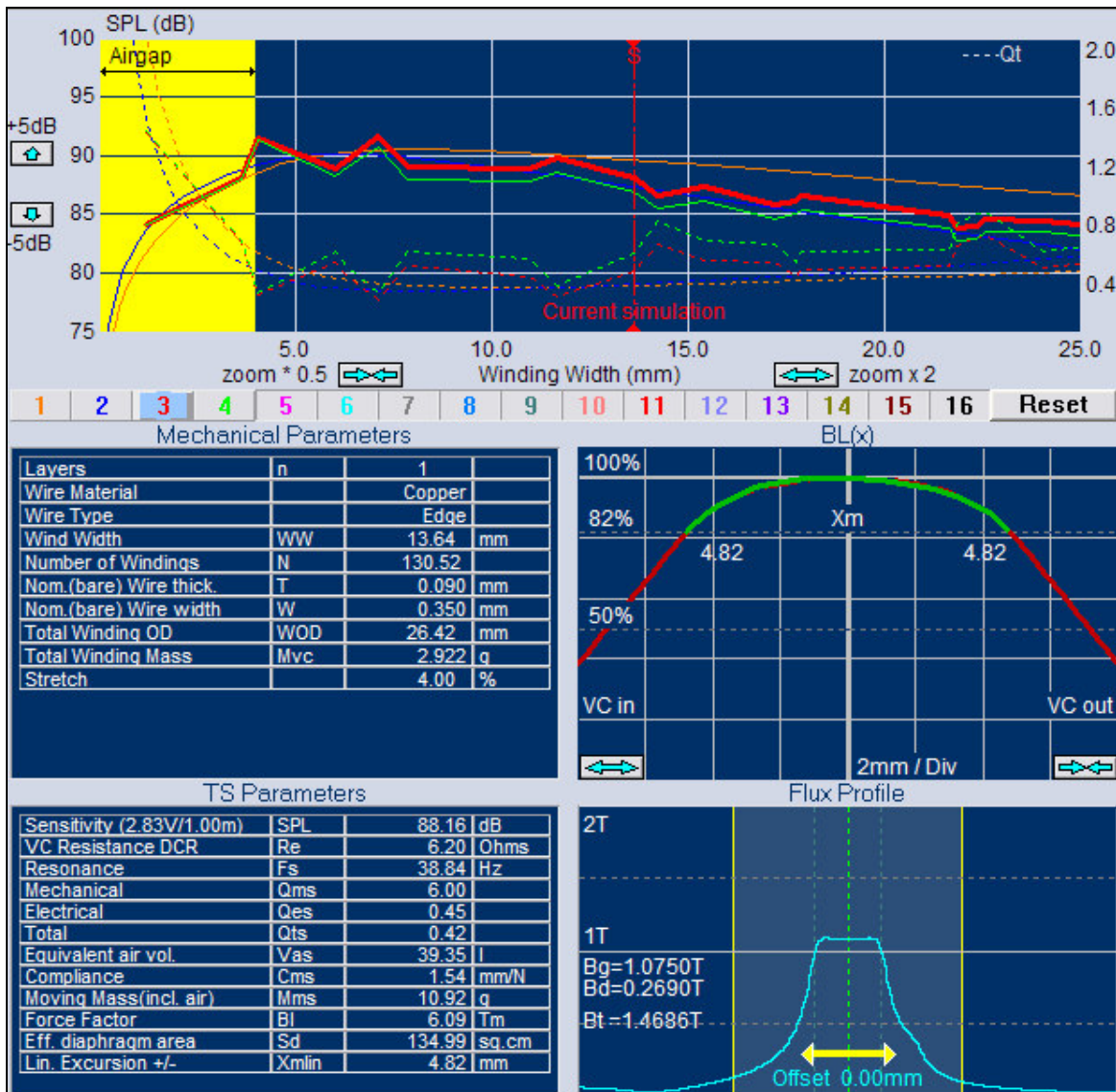


Figure 18 – Third Woofer Solution with 1-layer Flat Wire VC

The flat wire 1-layer VC is calculated in Fig. 18, indicated by the red simulation curve in the upper window. The actual wire is 0.09x0.35mm and the number of windings is down to 130, similar to the first 2-layer VC, which will ensure a low inductance.

The TS parameters are close to the target even with the smaller 72x32x15mm ferrite magnet, which is caused by the better fill factor of the flat wire.

In conclusion the low inductance designs are especially suited for mid-woofers and midranges, where the inductance distortion may be dominating. The multi-layer VC designs are well suited for subwoofers, however the BL and compliance symmetry is always important to avoid DC components and thereby distortion in the signal.



Figure 19 – Vifa Woofer P17WJ from 1987

The picture in Fig. 19 is the Vifa 6.5 inch P17WJ woofer, which was designed in 1987. The impedance curve in Fig 16 with the up/down VC position was actually measured from this driver. The 2-layer VC and undercut pole is the explanation for the little impedance variation.

Note the flat spider, which is progressive due to the sharp corrugations. There are exactly an integer number of full wave corrugations when the neck glue is assumed stiff.

Compliance with Gravity.

The total driver compliance will actually determine how far a woofer cone/VC will sink when placed horizontally. Therefore high compliant woofers with heavy cone/VCs may sink more than 1 mm. This is a simple calculation, actually the spider calculations in Fig. 11 can also be used here. Input the moving mass M_{ms} as load mass, and the C_{ms} as spider compliance, and the calculated deflection shows how many mm the cone will go down.

This was the reason for turning a large number of high compliant woofers upside down at Vifa many years ago. The cones had sunk too far while kept in stock.

Peter Larsen
LOUDSOFT

APPENDIX

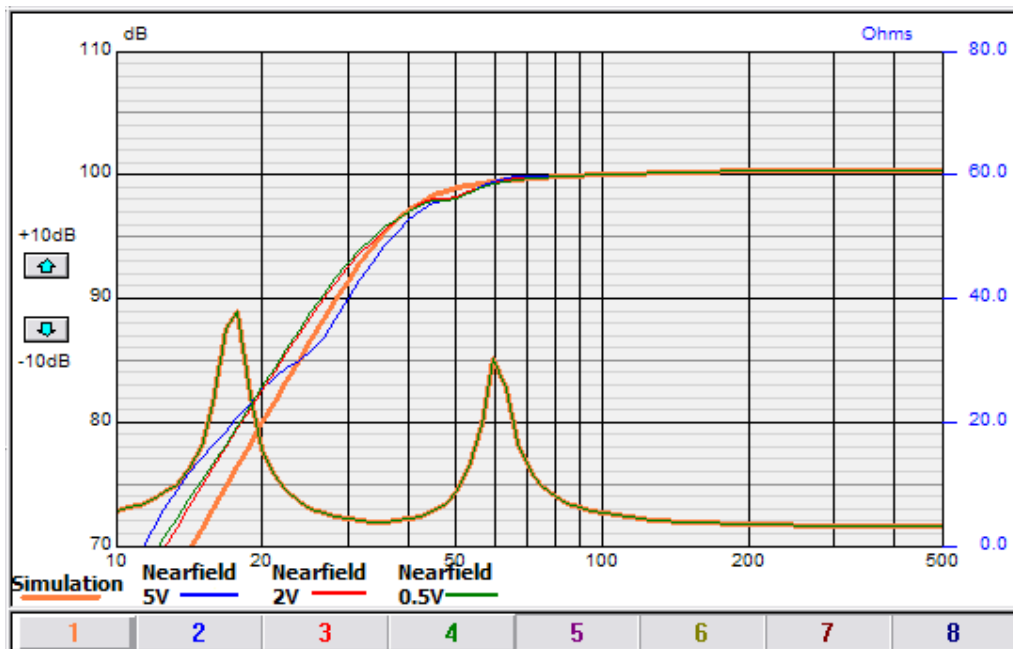


Figure 20 – 8in Bass Reflex System @ 0.5 / 2 / 5V Input

Finally an 8inch bass reflex subwoofer system was simulated. Following a real system was measured at different input levels 0.5, 2 and 5V to check the response variations, Fig. 20. The 0.5 and 2V responses are quite close to the simulated in the pass-band. Only the 5V curve is a little different mainly at very low frequencies below the cut-off frequency. The compliance curve of this driver was quite symmetrical but still quite progressive. Still the pass-band response was little affected by the suspension non-linearity.

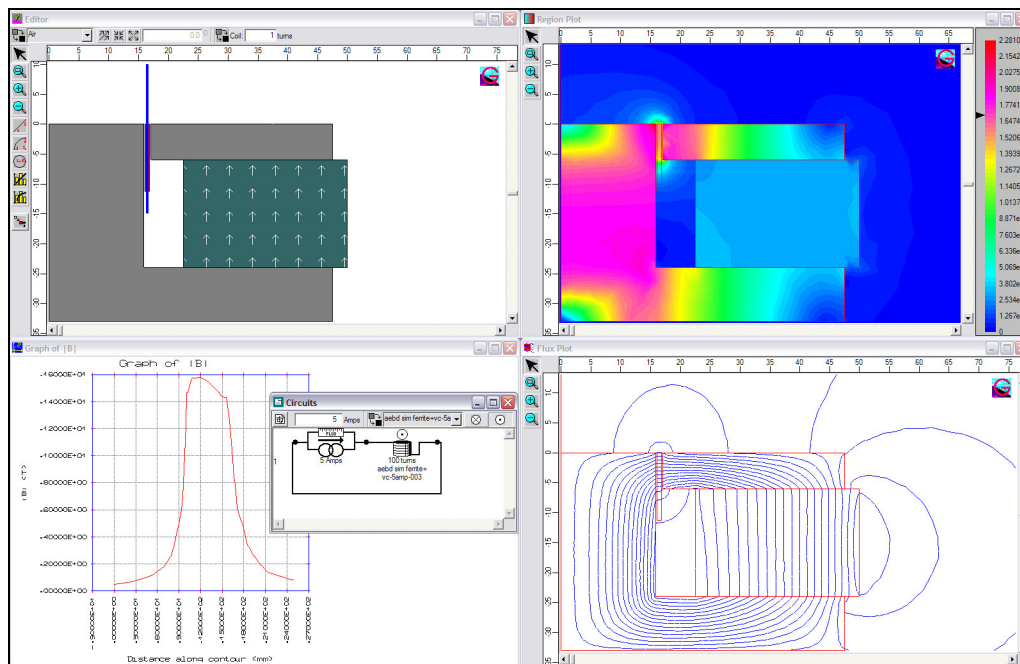


Figure 21 – High Current woofer Flux FEA Calculation

The last Fig. 21 shows a magnetic Finite Element Calculation of a high flux density ferrite motor with a Voice Coil having 100 windings while being run at 5 Amps peak current. There is no sign of demagnetization or saturation in the steel. This suggests that such phenomena may only happen in very extreme cases.

References

1. R. H. Small, Direct-Radiator Loudspeaker System Analysis, J. Audio Eng. Soc., vol. 20, pp. 383. 395 (1972 June).
2. R.H. Small, Closed-Box Loudspeaker Systems, Part I: Analysis, J. Audio Eng. Soc., vol. 20, pp. 798. 808 (1972 Dec.).
3. N. Thiele, Loudspeakers in Vented Boxes: Part I and II, in Loudspeakers, vol. 1 (Audio Eng. Society, New York, 1978).
4. W. Klippel, Nonlinear Large-Signal Behavior of Electrodynamic Loudspeakers at Low Frequencies, J. Audio Eng. Soc., vol. 40, pp. 483-496 (1992).
5. E. R. Olsen and K.B. Christensen, Nonlinear Modeling of Low Frequency Loudspeakers - a more complete model, presented at the 100th convention Audio Eng. Soc., Copenhagen, May 11-14, 1996, preprint 4205.
6. W. Klippel, "Diagnosis and Remedy of Nonlinearities in Electro-dynamical Woofers, presented at the 109th Convention of the Audio Engineering Society, Los Angeles, September 22-25, 2000, preprint 5261
7. P. Larsen, Better Speaker Designs in practice, LOUDSOFT, Oct 2007
8. P. Larsen, FINEMotor 2008 Tutorial, LOUDSOFT, Nov 2008
9. <http://en.wikipedia.org/wiki/Inductance>